Journal of Materials Chemistry C

Accepted Manuscript

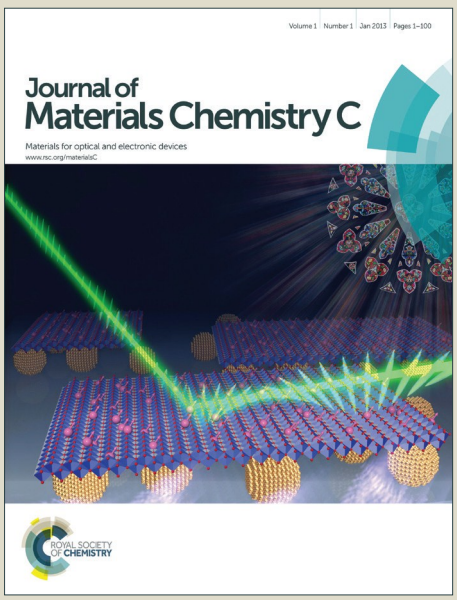

ROYAL SOCIETY OF CHEMISTRY

www.rsc.org/materialsC

Journal Name

ARTICLE

Greatly decreased redshift and largely enhanced refractive index of mono-dispersed ZnO-QD/silicone nanocomposites

Received 00th January 20xx,
Accepted 00th January 20xx

DOI: 10.1039/x0xx00000x

www.rsc.org/

Pei Huang,[a] Han-Qiao Shi,[b,§] Shao-Yun Fu,[a,*] Hong-Mei Xiao,[c] Ning Hu,[a,d] Yuan-Qing Li,[a,*]

The luminescence behavior of quantum dots (QDs) has been demonstrated to be size-dependent and the alternation of surroundings from solvent to matrix normally leads to large redshifts due to unavoidable occurrence of QD aggregates, which is detrimental to the successful application of QDs in light emitting devices (LEDs). In this work, a simple solvent mixing method is demonstrated to fabrication of transparent silicone nanocomposites with greatly decreased redshift and largely enhanced refractive index. By silane surface modification of ZnO-QDs, the dispersion of QDs in the silicone resin can be well controlled and the emission wavelength of QDs can be nearly precisely determined with a maximum redshift of 4 nm from ethanol solvent to silicone resin matrix. Compared to the un-modified ZnO QD case, the redshifts have been dramatically decreased. In addition, the as-fabricated ZnO-QD/silicone nanocomposites exhibit high visible light transparency while the diameter of ZnO-QDs varies from 1.8 nm to 4.5 nm. Meanwhile, by incorporation of ZnO-QDs at a low content up to 1.0 wt%, the refractive index of silicone resin is largely enhanced from 1.42 to 1.56. The current methodology is quality-controllable, cost-effective and environment-friendly and thus is applicable for the massive application of QD/silicone nanocomposites in LEDs.

1. Introduction

Owing to high color quality (saturated emission and precisely tunable peak emission wavelength),[1] wide range of excitation wavelength,[2] high efficiency,[3,4] energy-saving[5] and etc., quantum dots (QDs) have aroused great interests as a candidate for the fabrication of quantum dot-based light emitting devices (QD-LEDs) distinguished among the next generation lighting technology.[6] In recent years, tremendous advances in colloid chemistry have promoted the development of novel QDs based on varied elements, e.g. Cd,[7] Si,[8] carbon,[9] Zn[10] and etc. Many works have been devoted to lower the defect density in order to enhance the photoluminescence quantum yields and durability of QDs, such as surface passivized QDs with higher band gap inorganic materials[11] and metal doped QDs.[12]

When QDs are employed for the fabrication of LEDs, transparent polymers such as silicone and epoxy resins are usually used as encapsulating materials to protect the LED chip and to retain high transparency for light emission.[13-16] However, aggregation of QDs often takes place upon mixing QDs with polymers especially when the QD content is high. The compatibility between QDs and resin matrix is a serious issue to be solved for the performance of LEDs due to the fact that the aggregation of QDs in polymer matrices would result in detrimental effect on the luminescence behavior of QDs.[17] To overcome this problem, the conventional methods include surface passivation of QDs with organic layer,[18] polymer grafting,[19,20] alkoxysilane precursor containing a thiol group,[13] hybridization of QD/silica particles,[14] exfoliated nanoplatelets as an inorganic dispersant,[15] and so on. However, these protocols seemingly result in red-shift and poor quantum yield, ascribed to the absorption of polymer chain attached on the surface of QDs,[21,22] or the electronic energy transfer between QDs through long rang resonance.[23,24] The red-shift ranging from tens to 100 nm at different sized QDs[25-28] is un-predictable especially as the QD content increases, which is undesirable for LEDs. Although an increase in the diameter of QDs may reduce the redshift,[29] this protocol seems to be unable to realize the tunable emission wavelength of LEDs. So far, few literatures are focused on the redshift control over the luminescence behaviour of QDs.

In terms of packaging materials, silicone resin is taken to the priority option over epoxy resin because of its excellent thermal stability, high transparency and UV resistance.[30, 31] However, the high-refractive-index contrast between lighting chips (GaN~2.5) and silicone resin (typical silicone resin~1.44) greatly reduces the lighting efficiency. Although the bottom-up design of the polymer chain would increase the refractive index of silicone resin, the high cost and complex processing approach hinder its wide applications in LED fabrication.[32,33] In comparison, the introduction of inorganic

a College of Aerospace Engineering, Chongqing University, Chongqing 400044, China
b Aerospace Research Institute of Materials & Processing Technology, Beijing, 100190, China
c Technical Institute of Physics and Chemistry, Chinese Academy of Sciences, Beijing 100190, China
d The State Key Laboratory of Mechanical Transmissions, Chongqing University, Chongqing 400044, China
**Corresponding authors: syfu@cqu.edu.cn and yqli@cqu.edu.cn*
§ Equal contribution as first author

particles into resins has been proven to be a facile method to increase its refractive index.[34-36]

In our previous work, we have developed a novel method to synthesize ZnO-QDs via silanization during the growth process by (3-(2,3-epoxypropoxy)propyl)trimethoxysilane (KH-560), which was proven to have strong, tunable luminescence and enhanced quantum yields up to 30%.[37] The silane modified ZnO-QDs (S-ZnO-QDs) have shown a very stable luminescence behavior over several months. In addition, in comparison with other types of QDs, ZnO-QDs were featured for its nontoxicity and high stability towards air. These aforementioned properties are beneficial for the long-term service of Zn-QD-based LEDs. In this work, the S-ZnO-QDs are introduced into silicone resin to fabricate transparent silicone nanocomposites with controllable fluorescent property and largely enhanced refractive index. In order to evaluate the luminescence property of QDs, the luminescence behaviors of S-ZnO-QDs in ethanol suspension and silicone resin are characterized, respectively. Scanning electronic microscopy (SEM) and transmission electron microscope (TEM) are employed to investigate the dispersion of QDs in silicone resin. The transparency and refractive index (RI) of S-ZnO-QDs/silicone nanocomposites are examined taking into account the effects of QD size and loading.

2. Experiment section

2.1 Materials

Zinc acetate dehydrate ($Zn(CH_3COO)_2{\cdot}2H_2O$) and lithium hydroxide monohydrate ($LiOH{\cdot}H_2O$) were of analysis grade and obtained from Shantou Xilong Chemcial Reagent Company. Absolute ethanol, acetic ether, acetone, petroleum ether and cyclohexane, were supplied by Beijing Chemistry Reagent Company and used as received. KH-560 was purchased from Shanghai Yaohua Chemical Company. Silicone resin (KMT-1252, two parts) was purchased from KMT Technology Ltd.

2.2 Synthesis of S-ZnO-QDs

0.002 mol of $Zn(CH_3COO)_2{\cdot}2H_2O$ was dissolved in 20 mL absolute ethanol and the solution was refluxed at 80 ^oC for 2 h under continuous stirring. To synthesize silane surface modified ZnO QDs, the as-obtained solution was cooled to 0 ^oC in an ice water bath, and 0.6 mL KH-560 was added to the solution and intensely stirred for 20 minutes to ensure adequate dispersion. Meanwhile, a given amount of $LiOH{\cdot}H_2O$ was dissolved in ethanol by an ultrasonic technique and then cooled down to 0 ^oC. The Zn precursor and LiOH ethanol solution were mixed at a temperature of around 0 ^oC, followed by extensive stirring for 30 minutes to obtain a transparent colorless solution containing ZnO QDs. Four different sizes of ZnO QDs (denoted by A, B, C and D) were achieved under the molar ratio of $LiOH/Zn^{2+}$ with a value of 2.5, 1.9, 1.4 and 1.0 at the mixing temperature of 0 ^oC, respectively. In addition, to obtain silane surface modified ZnO QDs with longer wavelength (sample E), 100 mL of the Zn precursor was reacted with 1 ml of 10 M NaOH aqueous solution at 80 ^oC under vigorous stirring for 30 minutes.

2.3 Preparation of S-ZnO-QD nanocomposites

A certain amount of silicone resin (part A) was dispersed in 10 mL acetic ether by ultrasonic treatment until a transparent solution was obtained. Subsequently, a calculated amount of the as-prepared S-ZnO-QDs with various diameters in ethanol suspension was dispersed in the previous acetic ether solution by magnetic stirring for 30 min. The resulting suspension was added with curing agent of silicone resin (part B) by homogenously mixing. The mixture obtained was placed in a vacuum chamber for approximately 10 minutes to remove air bubbles, acetic ether and ethanol. The as-prepared suspension was then casted into a stainless steel mould and cured for 1 h at 80 ^oC and 1 h at 100 ^oC. Afterwards, the resulted nanocomposites were cooled at ambient atmosphere and ready to be characterized. The thickness of silicone composite specimens is approximately 1 mm.

2.4 Characterizations

Fourier transform infrared (FTIR) spectra were recorded using a Varian 3100 FT-IR spectrometer with 2 cm^{-1} resolution and accumulation of 24 scans. The luminescent spectra were measured by using a fluorescent photometer (Hitachi F-4600) with the excitation wavelength at 306 nm. Transmission electron microscope images were taken on a JEM-2100F instrument (operated at 200 kV). Scanning electron microscope images were collected on a Hitachi S-4300. The specimens were coated with gold by ion sputtering. The transmittance of the nanocomposite was measured by Hitachi U-3900. The RI was got on Abbe refractometer (WAY-2S) at room temperature.

3. Results and discussion

3.1 Synthesis of S-ZnO-QDs and silicone nanocomposites

The morphology of S-ZnO-QDs was characterized by TEM. As shown in **Figure 1A**, the as-prepared spherical S-ZnO-QDs are mono-dispersed in ethanol with a diameter of 1.8 nm. HRTEM image indicates that the lattice space between the two (002) planes of ZnO is 2.6 A˚ (bottom inset of **Figure 1A**). Additional evidence of FT-IR spectra demonstrates the formation of silane layer on the surface of ZnO cores. As shown in **Figure 1B**, in comparison with unmodified ZnO-QDs, there are newly emerged peaks around 2900 cm^{-1} and 1000 cm^{-1} assigned to C-H and Si-O bond, respectively. Moreover, S-ZnO-QDs have a significantly increased absorption at 3400 cm^{-1} ascribed to the vibration of O-H bonding. The aforementioned evidences indicate the successful synthesis of S-ZnO-QDs. Therefore, the same protocol was applied to synthesis of S-ZnO-QDs with a diameter of 2 nm, 2.2 nm, 3.3 nm and 4.5 nm, respectively, by varying the molar ratio of $LiOH/Zn^{2+}$.

The fabrication of S-ZnO-QD/silicone nanocomposite is illustrated in **Scheme 1**. S-ZnO-QDs were synthesized by sol-

gel method with the addition of silane coupling agent. The size of QDs was manipulated by controlling the ratio of LiOH/Zn^{2+}. Before mixing with S-ZnO-QD ethanol suspension, the silicone resin was diluted with acetic ether to reduce the viscosity and improve the miscibility of silicone resin with S-ZnO-QD ethanol suspension. After removing bubbles and solvent assisted by vacuum, the suspension obtained was cured at high temperature, giving desired specimens for further characterizations.

3.2 Luminescence behavior of ZnO-QDs

As shown in **Figure 2a**, with the increase of QD size, S-ZnO-QD/silicone nanocomposites display varied color from dark blue to yellow under the exposure of the UV light, indicating the strong size-dependence of luminescence behavior of QDs. To evaluate the effect of the QD size on the emission peaks of nanocomposites, the photoluminescence spectrum of S-ZnO-QD/silicone nanocomposite with the excitation wavelength at 302 nm was measured. As depicted in **Figure 2b**, while the diameter of QDs is sized at 1.8 nm, 2.0 nm, 2.2 nm, 3.3 nm and 4.5 nm, the emission peaks of the corresponding nanocomposite are located at 406 nm, 434 nm, 460 nm, 498 nm and 523 nm, respectively.

Table 1 Change of emission peaks of S-ZnO-QDs after being incorporated into silicone matrix.

Sample	1.8 nm	2.0 nm	2.2 nm	3.3 nm	4.5 nm
S-ZnO-QD in ethanol suspension	402 nm	431 nm	458 nm	496 nm	522 nm
S-ZnO-QD/silicone resin	406 nm	434 nm	460 nm	498 nm	523 nm

Table 1 shows the emission peaks of S-ZnO-QDs before and after being incorporated into the silicone matrix at the concentration of 1.0 wt%. For S-ZnO-QDs with a size of 1.8 nm, the emission peak of S-ZnO-QDs in ethanol and silicone matrix are 402 nm and 406 nm, respectively, indicating the redshift is only 4 nm. The increase in the diameter of ZnO-QDs further decreases the redshift. When the diameter of QDs increases up to 4.8 nm, the redshift of emission peak is only 1 nm. In comparison, redshifts of silicone nanocomposites based on unmodified ZnO-QDs[38] are much larger due to the aggregation of QDs in composite fabrication process. As shown in **Figure 3a**, for un-modified ZnO-QDs sized at 2, 3 and 4 nm, the resulted nanocomposites exhibit a redshift of 38, 7 and 18 nm,[38] respectively. This is the first time to report the ultra-small red-shifts of QD bulk nanocomposites. This results demonstrate the significant advantage of the current technology in precisely controlling the luminescence behavior. This tremendous improvement is attributed to the protective silane layer on the surface of ZnO-QDs, which avoids the aggregation of S-ZnO-QDs and results in an excellent and mono-dispersion of ZnO-QDs in silicone resin.

On the other hand, the loading of QDs plays an important role in the redshift of composite. As shown in **Figure 3b**, as the content of S-ZnO-QDs increases from 0.5 wt% to 5 wt%, the red-shift increases from 1 nm to 15 nm, which is attributed to the increased absorption by ZnO-QD aggregates caused by the decreased distance between neighboring QDs as demonstrated below by electron microscopy characterizations.[16,39-41] In comparison, ZnO-QDs stabilized by exfoliated Zirconium phosphate (ZrP) nanoplatelets exhibits much larger redshifts at similar ZnO-QD loadings.[42]

As shown in **Figure 4a** and **4b**, S-ZnO-QDs are uniformly dispersed in the silicone matrix when the content of S-ZnO-QDs is less than or equal to 1.0 wt%. This result is in agreement with that from TEM characterization (**Figure 5a** and **5b**), indicating an excellent dispersion of S-ZnO-QDs in the silicone matrix, self-explanatory of the minor redshift of the nanocomposite relative to the QDs in ethanol solution. This indicates that the dispersion state of S-ZnO-QDs in the silicone matrix can be controlled by the silane modification. This is understandable since the compatibility between S-ZnO-QDs and silicone matrix can be significantly improved by the silane treatment. Moreover, it should be noted that a further increase in the loading of QDs will lead to aggregates of QDs, which is undesirable for the luminescence behavior of LEDs. As shown in **Figure 4c** and **5c**, as the QD content increases up to 5.0 wt%, the QD aggregates occur in the silicone resin due to their large specific surface areas and short neighboring distances (**Figure 5d**) and this in turn would lead to relatively large res-shifts as shown in **Figure 3b**.

3.3 Transmittance of silicone nanocomposites

The transmittance of nanocomposite can be calculated by[43]

$$\frac{I}{I_0} = \exp\left\{\left[-\frac{32V_P x\pi^4 r^3}{\lambda^4}\left(\frac{(n_p/n_m)^2-1}{(n_p/n_m)^2+2}\right)^2\right]\right\} \qquad (1)$$

which applies to spherical particles with a radius of r and a RI of n_p uniformly dispersed in a matrix with a RI of n_m. I_0 is the intensity of light that would pass the sample without scattering, V_p is particle volume fraction, λ is light wavelength, and x *is* composite thickness. Since there is a big difference in the RI between ZnO-QDs and silicone resin,[44] the intensity loss by scattering in visible light range (400-800 nm) for the silicone nanocomposite becomes dominated for the particles with a diameter above 5–20 nm.[45] So, to obtain highly transparent silicone nanocomposites with a ZnO-QD loading around 1.0 wt%, it is necessary to ensure that all the ZnO-QDs are well dispersed in the silicone resin with a size of QDs or their aggregates well below 5 nm. As shown in **Figure 6a**, the S-ZnO-QD/silicone nanocomposite incorporated with 1.0 wt% of 1.8 nm S-ZnO-QDs exhibits approximately 88% transmittance in the wavelength range from 400 nm to 800 nm while 90% transmittance for the pure silicone resin. Below ca. 350 nm, the transmittance is sharply decreased due to the UV shielding effect of ZnO QDs. As the S-ZnO-QD size increases from 1.8 nm to 4.5 nm, the transmittance of the nanocomposites decreases but to a low degree. The transmittance of the nanocomposite with 4.5 nm S-ZnO-QDs still maintains at a high level of ca. 75%. This value is much higher than that of the nanocomposite incorporated with un-modified ZnO-QDs,[38] evidencing the excellent and mono-dispersion of S-ZnO-QDs in the

silicone resin. The transmittance of the un-modified ZnO-QD/silicone composites[38] was measured using the same device as done here for the S-ZnO-QD case.

Figure 6b shows that only a slight decrease is observed in transmittance when the loading of S-ZnO-QDs in composites is increased from 0.5 wt% to 1.0 wt%. However, when the S-ZnO-QD content is increased to 5.0 wt%, the transmittance of nanocomposite is dramatically decreased down to 20%, which is much lower than the value calculated from Equation 1. As proven by **Figures 4c and 5c,** this increased scattering should be caused by the formation of aggregates at a high loading of S-ZnO-QDs.

3.4 Refractive index of nanocomposites

It is well known that the difference of RI between LED chip and packaging materials leads to a great loss of lighting transmission, and thus a decrease of the lighting efficiency of LEDs. The incorporation of inorganic fillers is a facile method to increase the RI of packaging materials. According to Maxwell–Garnett effective medium theory[46, 47] (Equation 2), the mass fraction of ZnO-QDs determines the refractive index of ZnO-QD nanocomposites.

$$\frac{n_c^2-n_m^2}{n_c^2+2n_m^2} = \emptyset\left(\frac{n_{QD}^2-n_m^2}{n_{QD}^2+2n_m^2}\right) \qquad (2)$$

where n_c, n_{QD} and n_m are the RI of the nanocomposite, ZnO-QDs, and the silicone resin, respectively, and φ is the volume fractions of ZnO-QDs.

Figure 7a shows the RI of S-ZnO-QDs/silicone nanocomposite as a function of S-ZnO-QD content. As the S-ZnO-QD content increases, the RI of pure silicone resin is dramatically increased from 1.42 to 1.52 and 1.56 respectively at the loading of 0.5 wt% and 1.0 wt%. It should be noted that a further increase in the content of S-ZnO-QDs will decline this tendency. Only 4% increase in RI is obtained when the content of S-ZnO-QDs is increased from 1.0 wt% to 5.0 wt%, suggesting a limited enhancement at this level of S-ZnO-QDs. This is caused by the increased aggregation of S-ZnO-QDs, which increases the light scattering between S-ZnO-QDs and silicone resin. On the other hand, as the size of QDs increases, the refractive index of nanocomposite is almost not changed (**Figure 7b**), indicating no obvious dependence of RI on the QD size.

4. Conclusions

Silicone nanocomposites with greatly decreased redshift and largely enhanced refractive index have been fabricated by the incorporation of ultra-stable S-ZnO-QDs into the silicone resin. Owing to the protective silane layer on their surfaces, S-ZnO-QDs can be homogenously dispersed in the silicone resin via a simple direct mixing method. After the incorporation of S-ZnO-QDs into the silicone matrix, a maximum redshift of 4 nm is observed, which is much lower than that of the un-modified QD case. Meanwhile, the resulted nanocomposite maintains a high transparency at the loading of 1.0 wt%. Furthermore, the as-prepared nanocomposite is endowed with enhanced RI, which is useful to decrease the light scattering between LED chips and package materials. The aforementioned appealing features demonstrate that this new methodology has a great potential for application of S-ZnO-QD/silicone nanocomposites in LEDs of well-determined luminescence behavior.

Acknowledgements

This work is financially supported by National Natural Science Foundation of China (Nos. 51573200, 51373187, 11372312 and 11572321).

References

1. P. O. Anikeeva, J. E. Halpert, M. G. Bawendi and V. Bulovic, *Nano letters*, 2009, **9**, 2532-2536.
2. R. J. Ellingson, M. C. Beard, J. C. Johnson, P. Yu, O. I. Micic, A. J. Nozik, A. Shabaev and A. L. Efros, *Nano letters*, 2005, **5**, 865-871.
3. Y. Narukawa, M. Ichikawa, D. Sanga, M. Sano and T. Mukai, *Journal of physics D: Applied physics*, 2010, **43**, 354002.
4. Y. Yang, W. Chen, L. Dou, W.-H. Chang, H.-S. Duan, B. Bob, G. Li and Y. Yang, *Nat Photon*, 2015, **9**, 190-198.
5. H. Song and S. Lee, *Nanotechnology*, 2007, **18**, 255202.
6. E. Jang, S. Jun, H. Jang, J. Lim, B. Kim and Y. Kim, *Advanced Materials*, 2010, **22**, 3076-3080.
7. L. Qu and X. Peng, *Journal of the American Chemical Society*, 2002, **124**, 2049-2055.
8. K. D. Hirschman, L. Tsybeskov, S. P. Duttagupta and P. M. Fauchet, *Nature*, 1996, **384**, 338-341.
9. Y.-P. Sun, B. Zhou, Y. Lin, W. Wang, K. A. S. Fernando, P. Pathak, M. J. Meziani, B. A. Harruff, X. Wang, H. Wang, P. G. Luo, H. Yang, M. E. Kose, B. Chen, L. M. Veca and S.-Y. Xie, *Journal of the American Chemical Society*, 2006, **128**, 7756-7757.
10. Y.-S. Fu, X.-W. Du, S. A. Kulinich, J.-S. Qiu, W.-J. Qin, R. Li, J. Sun and J. Liu, *Journal of the American Chemical Society*, 2007, **129**, 16029-16033.
11. B. Dabbousi, J. Rodriguez-Viejo, F. V. Mikulec, J. Heine, H. Mattoussi, R. Ober, K. Jensen and M. Bawendi, *The Journal of Physical Chemistry B*, 1997, **101**, 9463-9475.
12. P. K. Santra and P. V. Kamat, *Journal of the American Chemical Society*, 2012, **134**, 2508-2511.
13. C. Yoon, T. Kim, M. H. Shin, Y. G. Song, K. Shin, Y. J. Kim and K. Li, *Journal of Materials Chemistry C*, 2015, **3**, 6908-6915.
14. H. C. Kim, H. G. Hong, C. Yoon, H. Choi, I. S. Ahn, D. C. Lee, Y. J. Kim and K. Lee, *Journal of Colloid Interface Science*, 2013, **393**, 74–79.
15. D. Z. Sun and H. J. Sue, *Applied Physics Letters*, 2009, **94**, 253106.
16. Y. Yang, Y. Q. Li, H. Q. Shi, W. N. Li, H. M. Xiao, L. P. Zhu, Y. S. Luo, S. Y. Fu and T. X. Liu, *Composites Part B Engineering*, 2011, **42**, 2105-2100.
17. M. V. Artemyev, A. I. Bibik, L. I. Gurinovich, S. V. Gaponenko and U. Woggon, *Physical Review B*, 1999, **60**, 1504-1506.
18. H. Song and S. Lee, *Nanotechnology*, 2007, **18**, 055402.
19. P. Tao, Y. Li, R. W. Siegel and L. S. Schadler, *Journal of Materials Chemistry C*, 2013, **1**, 86-94.
20. A. Cosgun, R. Fu, W. Jiang, J. Li, J. Song, X. Song and H. Zeng, *Journal of Materials Chemistry C*, 2015, **3**, 257-264.
21. H.-M. Xiong, X. Zhao and J.-S. Chen, *The Journal of Physical Chemistry B*, 2001, **105**, 10169-10174.

22. R. P. Pereira, A. M. Rocco and C. E. Bielschowsky, *The Journal of Physical Chemistry B*, 2004, **108**, 12677-12684.
23. C. R. Kagan, C. B. Murray and M. G. Bawendi, *Physical Review B*, 1996, **54**, 8633-8643.
24. C. R. Kagan, C. B. Murray, M. Nirmal and M. G. Bawendi, *Physical Review Letters*, 1996, **76**, 1517-1520.
25. J. Huang, K. Sooklal, C. J. Murphy and H. J. Ploehn, *Chemistry of Materials*, 1999, **11**, 3595-3601.
26. J.-H. Kim, W.-S. Song and H. Yang, *Opt. Lett.*, 2013, **38**, 2885-2888.
27. F. Iskandar, K. Okuyama and F. Shi, *Journal of Applied Physics*, 2001, **89**, 6431-6434.
28. Y. Yang, H.-Q. Shi, W.-N. Li, H.-M. Xiao, Y.-S. Luo, S.-Y. Fu and T. Liu, *Composites Science and Technology*, 2011, **71**, 1652-1658.
29. Y. Yang, Y.-Q. Li, H.-Q. Shi, W.-N. Li, H.-M. Xiao, L.-P. Zhu, Y.-S. Luo, S.-Y. Fu and T. Liu, *Composites Part B: Engineering*, 2011, **42**, 2105-2110.
30. M. Arik, A. Setlur, S. Weaver, D. Haitko and J. Petroski, *Journal of Electronic Packaging*, 2007, **129**, 328-338.
31. T. Maehara, J. Takenaka, K. Tanaka, M. Yamaguchi, H. Yamamoto and J. Ohshita, *Journal of Applied Polymer Science*, 2009, **112**, 496-504.
32. D. W. Mosley, G. Khanarian, D. M. Conner, D. L. Thorsen, T. Zhang and M. Wills, *Journal of Applied Polymer Science*, 2014, **131**, 39824-39834.
33. X. Yang, Q. Shao, L. Yang, X. Zhu, X. Hua, Q. Zheng, G. Song and G. Lai, *Journal of Applied Polymer Science*, 2013, **127**, 1717-1724.
34. P. T. Chung, C. T. Yang, S. H. Wang, C. W. Chen, A. S. T. Chiang and C.-Y. Liu, *Materials Chemistry and Physics*, 2012, **136**, 868-876.
35. P. Tao, Y. Li, A. Rungta, A. Viswanath, J. Gao, B. C. Benicewicz, R. W. Siegel and L. S. Schadler, *Journal of Materials Chemistry*, 2011, **21**, 18623-18629.
36. Y. He, J.-A. Wang, C.-L. Pei, J.-Z. Song, D. Zhu and J. Chen, *Journal of Nanoparticle Research*, 2010, **12**, 3019-3024.
37. H.-Q. Shi, W.-N. Li, L.-W. Sun, Y. Liu, H.-M. Xiao and S.-Y. Fu, *Chemical Communications*, 2011, **47**, 11921-11923.
38. Y. Yang, W.-N. Li, Y.-S. Luo, H.-M. Xiao, S.-Y. Fu and Y.-W. Mai, *Polymer*, 2010, **51**, 2755-2762.
39. L. Spanhel and M. A. Anderson, *Journal of the American Chemical Society*, 1991, **113**, 2826-2833.
40. C. Kagan, C. Murray and M. Bawendi, *Physical Review B*, 1996, **54**, 8633.
41. C. Kagan, C. Murray, M. Nirmal and M. Bawendi, *Physical Review Letters*, 1996, **76**, 1517.
42. D. Sun, H.-J. Sue and N. Miyatake, *The Journal of Physical Chemistry C*, 2008, **112**, 16002-16010.
43. B. M. Novak, *Advanced Materials*, 1993, **5**, 422-433.
44. A. Ashrafi and C. Jagadish, *Journal of Applied Physics*, 2007, **102**, 071101.
45. W. Caseri, *Materials Science and Technology*, 2006, **22**, 807-817.
46. J. M. Garnett, *Proceedings of the Royal Society of London*, 1904, 443-445.
47. D. E. Aspnes, *American Journal of Physics*, 1982, **50**, 704-709.

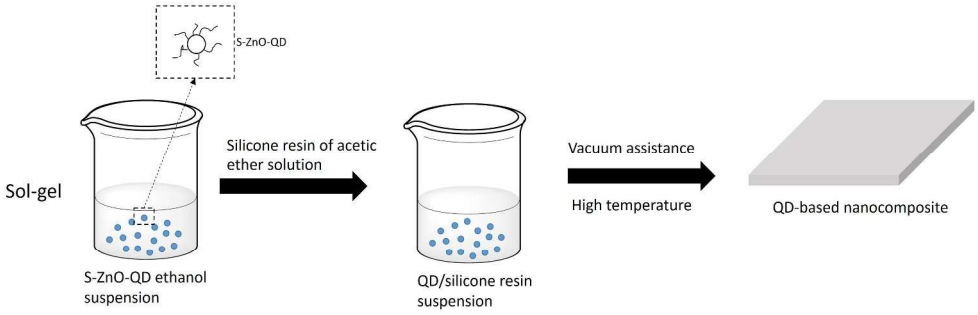

Scheme 1 Illustration of nanocomposite processing procedure.
Scheme 1
338x130mm (300 x 300 DPI)

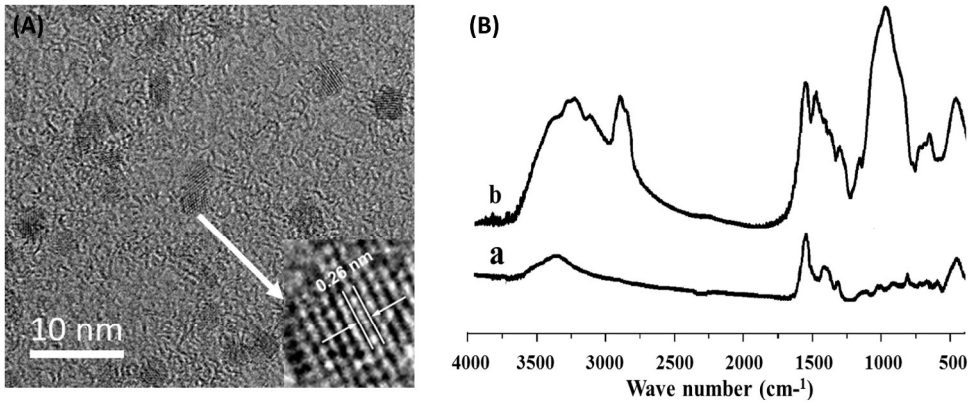

Figure 1 (A) TEM image of S-ZnO-QDs (bottom inset: HRTEM image of S-ZnO-QDs); (B) FT-IR spectrum of (a) unmodified ZnO-QDs and (b) S-ZnO-QDs.
Figure 1
325x142mm (300 x 300 DPI)

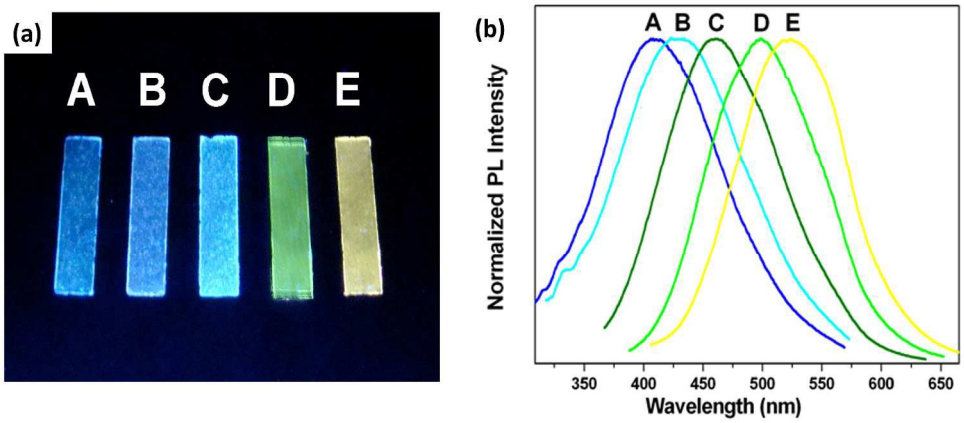

Figure 2 (a) Digital photographs and (b) photoluminescence spectra of 1 wt% S-ZnO-QD/silicone bulk composites with different sizes of S-ZnO-QDs under 302 nm UV light irradiation: (A) 1.8 nm, (B) 2.0 nm, (C) 2.2 nm, (D) 3.3 nm, and (E) 4.5 nm.
Figure 2
316x139mm (300 x 300 DPI)

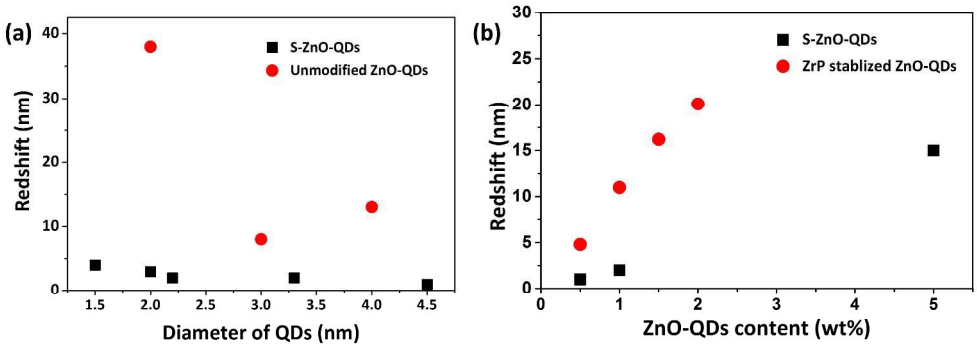

Figure 3 (a) Comparison of redshift in emission peaks of 1 wt% S-ZnO-QDs and unmodified ZnO-QDs [38] after being incorporated into the silicone matrix, (b) redshift of silicone composites with 4.5 nm ZnO-QDs and epoxy composites with ZnO-QDs stabilized by ZrP [42] as a function of ZnO-QD content.
Figure 3
338x190mm (300 x 300 DPI)

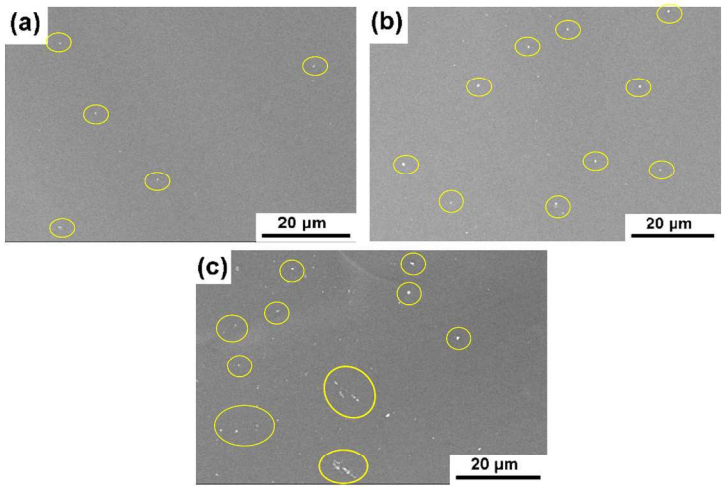

Figure 4 SEM images of the cross sections of S-ZnO-QD/silicone nanocomposites with different S-ZnO-QD contents: (a) 0.5 wt%, (b) 1.0 wt%, and (c) 5.0 wt%, and the diameter of S-ZnO-QDs is ca. 4.5 nm.
Figure 4
338x190mm (300 x 300 DPI)

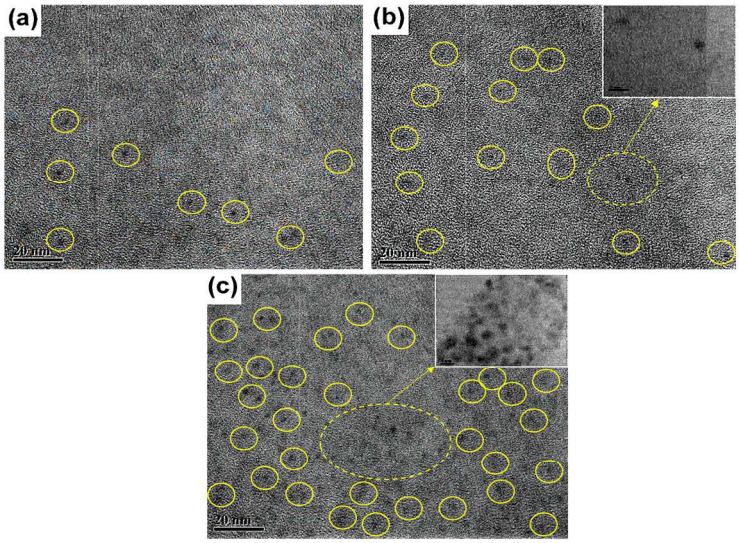

Figure 5 TEM images of the cross sections of S-ZnO-QD/silicone nanocomposites with different S-ZnO-QD contents: (a) 0.5 wt%, (b) 1 wt% (top inset: higher magnification of S-ZnO-QDs), and (c) 5 wt%, and the diameter of S-ZnO-QDs in the nanocomposites is 4.5 nm (top inset: higher magnification of S-ZnO-QDs).
Figure 5
338x190mm (300 x 300 DPI)

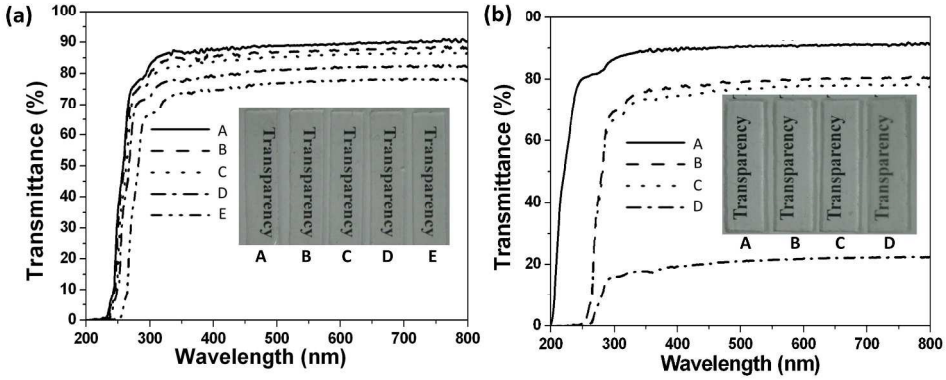

Figure 6 Transmittance of S-ZnO-QD/silicone nanocomposites containing QDs of (a) different sizes: (A) 1.8 nm, (B) 2.0 nm, (C) 2.2 nm, (D) 3.3 nm, and (E) 4.5 nm (the content of S-ZnO-QDs is fixed at 1 wt%), as well as (b) different contents: (A) 0.0 wt%, (B) 0.5 wt%, (C) 1.0 wt%, and (D) 5.0 wt% (the size of S-ZnO-QDs is fixed as 4.5 nm).

Figure 6

338x190mm (300 x 300 DPI)

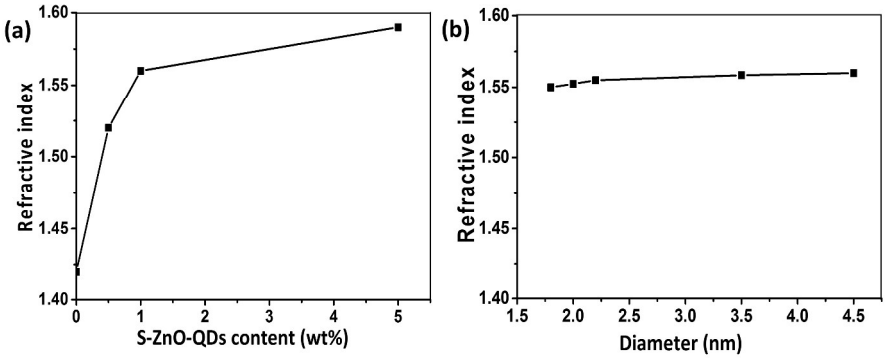

Figure 7 RI of S-ZnO-QDs/silicone nanocomposites with different loading (a) of S-ZnO-QDs sized 1.8 nm and different particle size (b) of ZnO-QDs.
Figure 7
338x190mm (300 x 300 DPI)

Abstract

The luminescence behavior of quantum dots (QDs) has been demonstrated to be size-dependent and the alternation of surroundings from solvent to matrix normally leads to large redshifts due to unavoidable occurrence of QD aggregates, which is detrimental to the successful application of QDs in light emitting devices (LEDs). In this work, a simple solvent mixing method is demonstrated to fabricate silicone nanocomposites with a mono-dispersion of Zn-QDs in the silicone resin. By silane surface modification of ZnO-QDs, the dispersion of QDs in the silicone resin can be well controlled and the emission wavelength of QDs can be nearly precisely determined with a maximum redshift of 4 nm from ethanol solvent to silicone resin matrix. Compared to the un-modified ZnO QD case, the redshifts have been dramatically decreased. In addition, the as-fabricated ZnO-QD/silicone nanocomposites exhibit high visible light transparency while the diameter of ZnO-QDs varies from 1.8 nm to 4.5 nm. Meanwhile, by incorporation of ZnO-QDs at a low content up to 1 wt%, the refractive index of silicone resin is largely enhanced from 1.42 to 1.56. The current methodology is quality-controllable, cost-effective and environment-friendly and thus is applicable for the massive application of QD/silicone nanocomposites in LEDs.